ELSEVIER

Journal of Marine Systems 37 (2002) 31–46

JOURNAL OF MARINE SYSTEMS

www.elsevier.com/locate/jmarsys

Diapycnal flow through a tidal front: a dye tracer study on Georges Bank

Robert W. Houghton*

Lamont-Doherty Earth Observatory of Columbia University, 202 Oceanography Rt 9W, Palisades, NY 10964, USA

Received 18 January 2001; received in revised form 28 November 2001; accepted 28 November 2001

Abstract

A fluorescent dye tracer, fluorescein, injected into the bottom mixed layer (BML) at the off-bank edge of the tidal front on Georges Bank in late May and early June 1999 has provided the first quantitative measurement of an on-bank diapycnal Lagrangian flow through the front. From the warming of the dye patch, 1.9×10^{-6} and 7.6×10^{-6} °C/s on the south flank and northeast peak, respectively, as it passed through the frontal temperature gradient, we infer a mean on-bank flow of 1.6 cm/s on the south flank and 3.1 cm/s on the northeast peak. The heat flux required for this warming is predominantly due to vertical mixing within the tidal front. From the dispersion of the dye patch, we estimate a vertical diffusivity of 1.6 and 3.1×10^{-3} m^2/s and a cross-front diffusivity of 18 and 30 m^2/s on the south flank and northeast peak, respectively.

The evolution of a second dye injection on the south flank was distinctly different from the first because of the proximity of the foot of shelfbreak front now displaced onto the bank by a transient meander to within 6 km of the tidal front. Although the dispersion of this patch was the same as for the first injection, its cross-bank displacement was much less reflecting the divergence of the cross-bank flow in this region.

Keywords: Diapycnal flow; Dye tracer; Tidal front

1. Introduction

The tidal front surrounding Georges Bank (Fig. 1) defined as the transition region separating stratified and vertically mixed water, is generated by the predominately M_2 tide with amplitudes up to 1 m/s. On the south flank, the tidal front located between the 40 and 60 m isobath, is distinct from the shelfbreak front whose foot is at the 100 m isobath. On the north flank where changes in bottom topography are more abrupt, the two frontal features are merged.

Tidal rectification generates a cyclonic jet at the bank edge and a cross-bank flow through the tidal front (Garrett et al., 1978; Garrett and Loder, 1981; Loder et al., 1992), both of which are intensified during the more stratified summertime. The general features of the along-bank circulation have been successfully modeled (Butman and Beardsley, 1987; Chen et al., 1995; Lynch et al., 1996) and observed (Butman and Beardsley, 1987; Limeburner and Beardsley, 1996; Loder and Wright, 1985). In con-

* Fax: +1-845-365-8157.
E-mail address: houghton@ldeo.columbia.edu (R.W. Houghton).

0924-7963/02/$ - see front matter © 2002 Elsevier Science B.V. All rights reserved.
PII: S0924-7963(02)00194-X

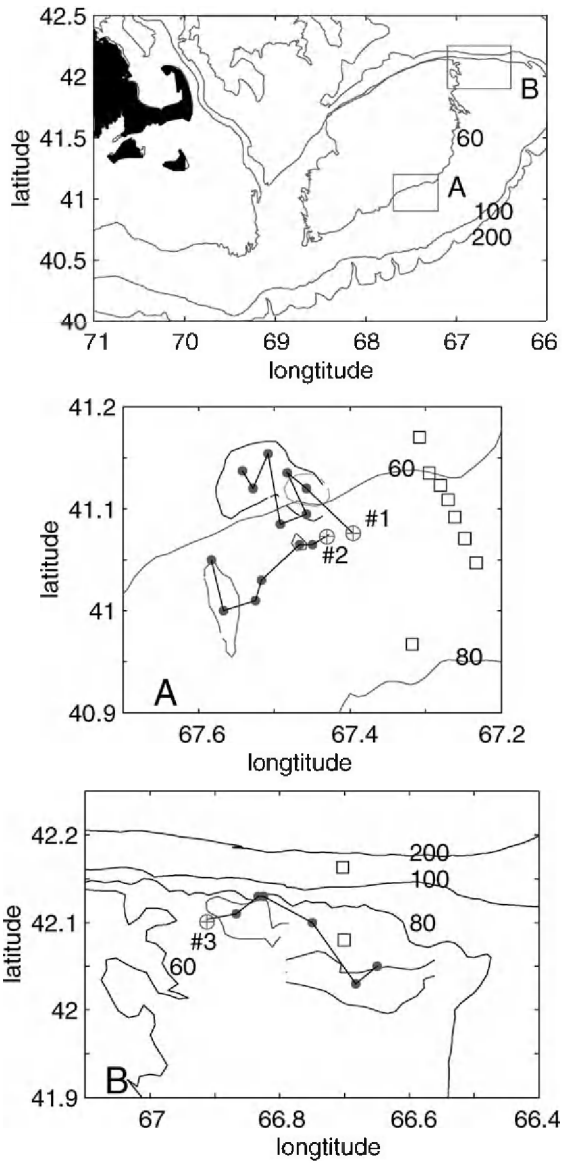

Fig. 1. Location of the study site on Georges Bank on the south flank (box A) and the northeast peak (box B). Box A: Detail of the isobaths and the GLOBEC current meter mooring sites (□) in the vicinity of the dye injection. The tidal front is roughly parallel to the local isobath. Dye injection site denoted by ⊕ and the centroid of subsequent patch surveys by ●. Aliasing by tidal motion is evident. The shape of the dye patch during the first and last survey is given by the locus where the depth-integrated dye content is $1/e$ of the maximum value at the center. Box B: Same as for A. Here the tidal front extends eastward in a region where local isobaths are turning south. Gaps in the patch outline are where the survey did not fully extend to the edge of the patch.

trast, there have been no direct measurements of a significant non-zero mean cross-bank flow. There are several reasons for this. The anticipated speed, 1–3 cm/s, is small compared to the mean along-bank flow, 15–40 cm/s, and very small compared to tidal speeds. Eulerian measurements of this flow are not feasible since the front is not always aligned along the local isobath, the front undergoes tidally driven cross-bank displacements (7–10 km) comparable with its width, and Stokes terms are large such that on the northern flank, the Lagrangian and Eulerian velocities may be of opposite sign.

This cross-bank flow is a potentially important mechanism affecting cross-frontal exchange, the focus of the U.S. GLOBEC Northwest Atlantic/Georges Bank Program, phase III. Therefore, a Lagrangian approach, the tracking of a purposeful tracer, was proposed. We report here the results of dye tracer releases into the bottom mixed layer (BML) at the tidal front, which for the first time give quantitative estimates of the on-bank flow through the tidal front on Georges Bank.

2. Experiment

The experiment consisted of tracking a dispersing patch of water tagged with a fluorescent dye that was injected into the BML on the off-bank side of the tidal front. There were three dye injections, two on the south flank of Georges Bank and one on the northeast peak (Fig. 1). Each injection consisted of pumping 86 kg of fluorescein dye in a 25% water solution, mixed with isopropyl alcohol to achieve in situ density, into a well-mixed BML through a garden hose in 40 min during slack cross-bank tidal flow to produce a streak of dye approximately 0.5 km long.

The dye was detected using a Chelsea Instruments Aquatracka MKIII fluorometer sampled at 2 Hz. Dye was detectable to dilutions of 1×10^{-11} parts by weight, which was the level of the background signal. The fluorometer was mounted on a Scanfish, a towed undulating vehicle, provided by the University of Rhode Island, which was equipped with a Sea Cat SBE 19 CTD. The surveys of the dye patch were conducted by towing the Scanfish at 6 knots while it undulated vertically between 5 and 10 m below the surface and above the bottom. The dye patch (Fig. 1)

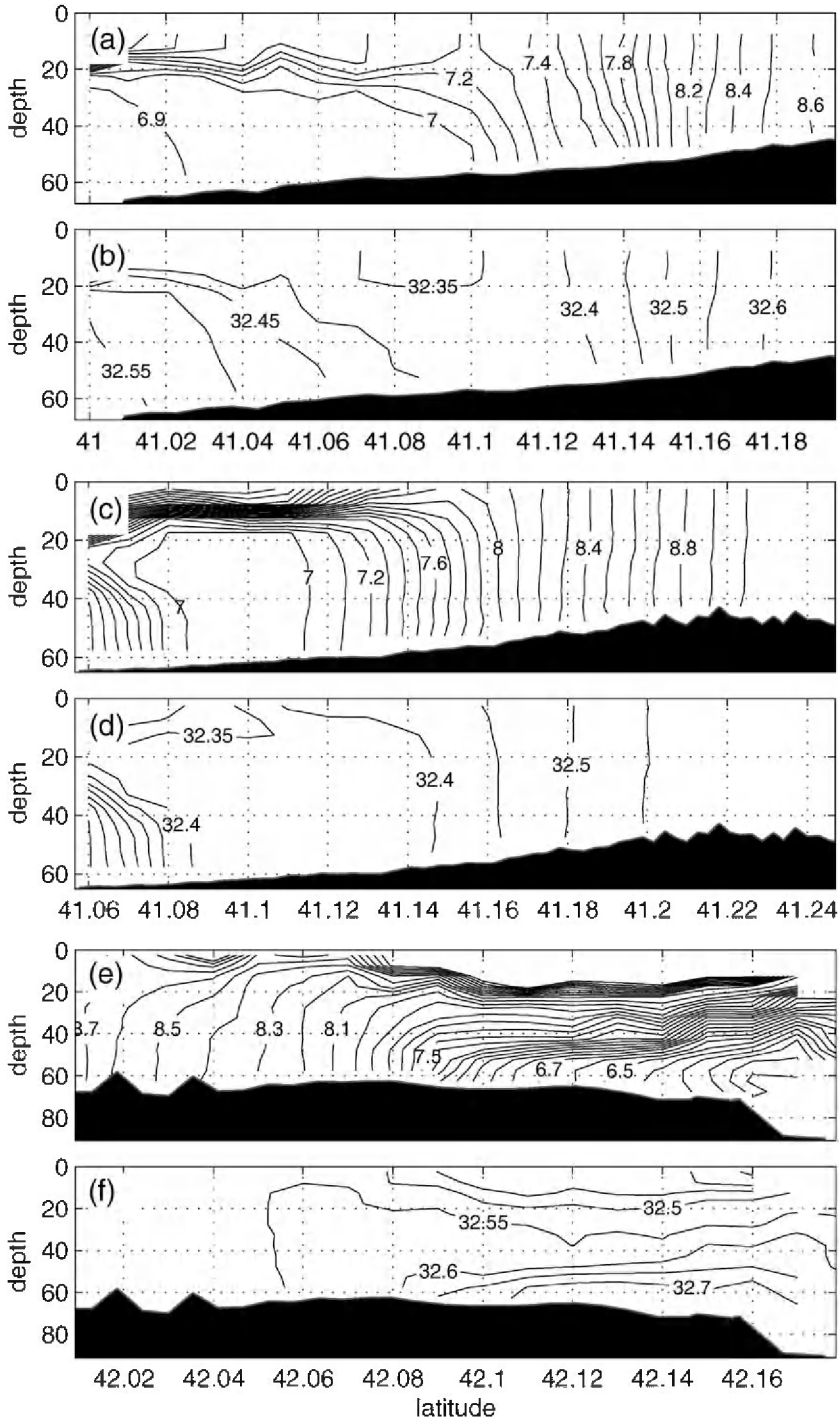

Fig. 2. Cross-bank sections of temperature (a, c, and e) and salinity (b, d, and f) taken prior to the three dye injections: #1 (a and b), #2 (c and d), #3 (e and f).

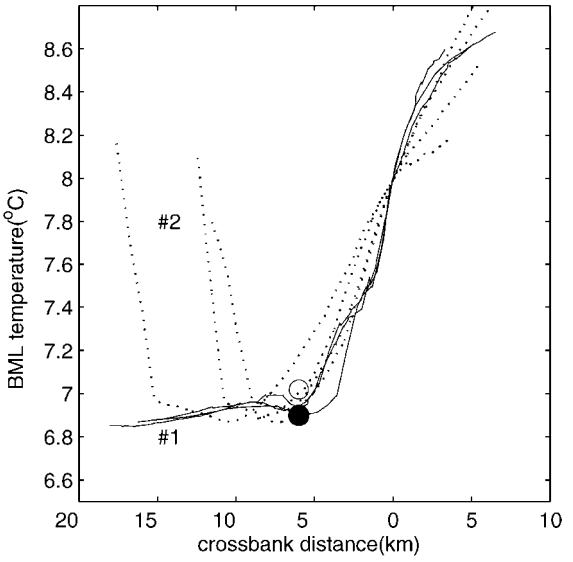

Fig. 3. BML temperature, as a function of cross-bank distance, derived from the cross-front temperature sections prior to injection #1 (solid line) and #2 (dotted line). North is positive. Curves are shifted to coincide at 8 °C. Anticipated dye injection location indicated by ● for #1 and ○ for #2.

was defined by a survey consisting of at least six cross-bank sections through the patch with successive up traces separated by 500 m and with a vertical resolution of 0.25 m.

The horizontal displacement of the water column was estimated by integrating velocity data from the ship mounted ADCP. This was used to predict the initial displacement of the dye patch after injection, to survey the patch with approximately evenly spaced sections, and to adjust the data position within each survey to a common reference time for subsequent analysis to minimize the spatial distortion due to water motion.

Prior to each dye injection, cross-bank hydrographic surveys (Fig. 2) were conducted to locate the front and to identify an optimal injection location. For injection #1 on the south flank, stratification was primarily the result of surface heating. The tidal front was situated between 7.0 and 7.8 °C although horizontal gradients in the vertically mixed region extended further onto the bank. For injection #2, also on the south flank, the stratification had increased due to continued surface heating and to an intrusion of the foot of the shelfbreak front from offshore. Satellite (SST) images (courtesy of J. Bisagni) indicate that this was due to a meander of the shelfbreak front that was drifting westward through the study area. For injection #3, on the northeast peak, vertical and horizontal temperature and salinity gradients are greater and the frontal structure more complex. Here the tidal front extends approximately from 6.0 to 8.3 °C although some patches of stratification due to intense local heating persist near the surface over the bank.

The horizontal temperature gradient in the BML, derived from these surveys on the south flank, is shown in Fig. 3. The curves are laterally displaced to a common origin at 8.0 °C. In spite of small-scale temporal and spatial variabilities in the magnitude of the local temperature gradient, the abrupt increase in the temperature gradient on the seaward side of the tidal front is distinct. The location of this change was identified to establish the location of the subsequent dye injection.

All three dye injections (Table 1) were in a thick BML such that the variation of the in situ temperature and salinity values during injection was due only to ship drift through lateral gradients. Injection #1 was located at the off-bank edge of the tidal front (Fig. 3). Although the location of injection #2 with respect to the tidal front was similar, it was located near a local temperature minimum due to the proximity of the shelfbreak front offshore. Injection #3 was inside of the off-bank edge of the tidal front since during the large off-bank tidal excursion, this water was displaced to depths that could not easily be sampled by the Scanfish. Surveys of the dye patch were repeated until the signal-to-noise ratio at the center of the patch was reduced to 3, which occurred approximately 96 h after injection on the south flank and 60 h on the northeast peak (Fig. 4). At this time, the quantity of

Table 1
Dye injection parameters

Injection	#1	#2	#3
Date	22 May	27 May	2 June
Latitude	41°4.58′ N	41°4.50′ N	42°6.21′ N
Longitude	67°23.17′ W	67°25.69′ W	66°54.81′ W
Bottom depth (m)	63	63	66
BML thickness	24	30	26
Depth above bottom	5	6	6
Temperature (°C)	6.87–6.96	7.00–7.02	6.84–6.85
Salinity	32.38–32.37	32.354–32.355	32.67

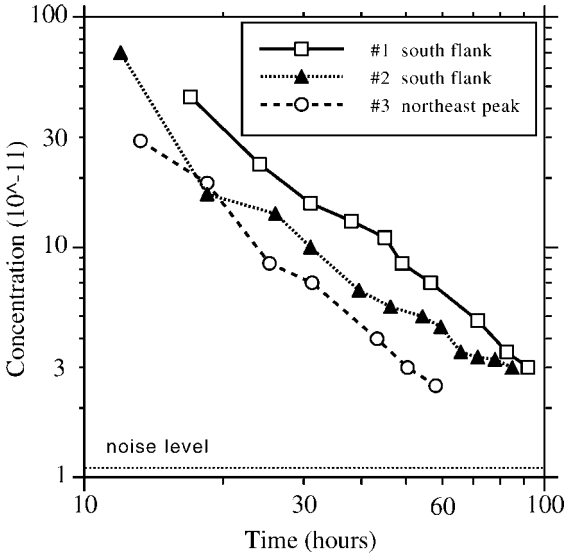

Fig. 4. Maximum dye concentration within the patch as a function of time after injection.

dye within the observed patch was between 50% and 90% of the injected amount so the surveys provided representative sampling of the evolution of the dye-tagged water.

3. Observations

The lateral displacement and spreading of the dye patches is illustrated in Fig. 1 where the circles represent the center of the patch defined by successive surveys. Although aliasing by tidal motion results in considerable scatter in the position of the patch centroid, the drift of the patch is clearly evident. The mean along-front drift is 4.1, 6.3, and 11.0 cm/s for #1, #2, and #3, respectively. The cross-frontal motion is more difficult to discern since it is smaller and since the tidal front, especially on the northeast peak, is not necessarily aligned with the local isobath. On the south flank, however, patch #1 clearly has a greater on-bank displacement than #2.

3.1. Dye patch displacement

The cross-frontal motion is determined more precisely relative to the isotherms (isopycnals) that define the front. Successive cross-bank sections through the center of the dye patches (Fig. 5) illustrate the on-bank flow of dye-tagged water through the tidal front. Fig. 5a shows a section through #1 16 h after injection. The middle of the patch, now centered at 7 °C, has clearly been displaced on-bank from its injection position, indicated by the crossed circle. Eighty-five hours after injection (Fig. 5b), there is no dye at the injection temperature and the maximum dye concentration is at 7.6 °C.

The same warming and, hence, on-bank flow is observed with #3 on the northeast peak. Twelve hours after injection (Fig. 5e), there is significant diathermal (diapycnal) displacement of the patch to warmer temperatures. Although there is a suggestion of isothermal (isopycnal) spreading, it is the diathermal changes that predominate in the cross-bank direction. Nearly all of the dye-tagged water has moved on-bank of the tidal front 55 h after injection (Fig. 5f) and the patch is now centered at 8.4 °C, with virtually none remaining at the injection temperature of 6.85 °C.

The evolution of #2 on the south flank was distinctly different from #1. Within a few hours after injection, the dye-tagged water shoaled along sloping isotherms to the base of the pycnocline (Fig. 5c) 40 m above the bottom. The center of the entire patch was located at the base of the pycnocline. Apparently this motion was forced by a complex 3-D circulation associated with the intrusion of the foot of the shelf-slope front from the southeast. Subsequently the dye mixed isothermally throughout the water column (Fig. 5d) and then began a diathermal flow on-bank into the tidal front.

3.2. T/S property evolution

The evolution of the water properties of the three dye patches is illustrated in the *T/S* diagram in Fig. 6. The patch averaged temperature and salinity is superposed on *T/S* curves defined by the data from a preinjection section across the tidal front and onto the cap of the bank (Fig. 2). These data illustrate both the vertical and horizontal gradients in the vicinity of the front. The lateral *T/S* changes on the well-mixed side of the front on the south flank are given by the curves that are well defined by the densely spaced data. Also evident is the shelfbreak front incursion prior to injection #2 (the green data) and the seasonal

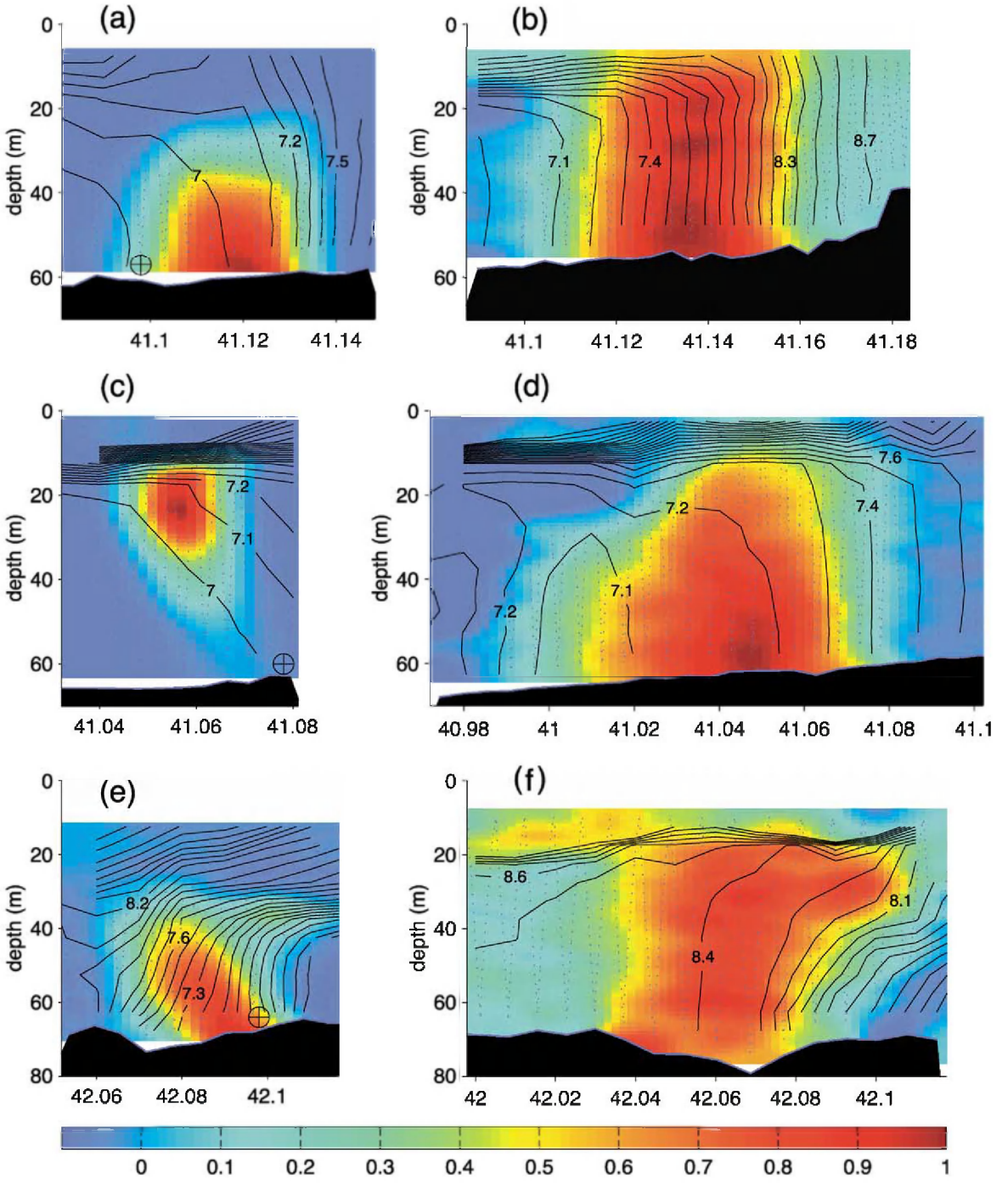

Fig. 5. Cross-front sections of dye concentration, normalized by the maximum value in each section, through the center of the dye patch at the denoted times after injection for: #1 (a) 16 h and (b) 85 h, #2 (c) 10 h and (d) 66 h, and #3 (a) 12 h and (b) 55 h. The relative location of the dye injection site is given by ⊕ and the Scanfish track by the dotted line. Temperature contour interval is 0.1 °C. In e and f, on-bank direction through the tidal front is to the left even though the local bathymetry is level.

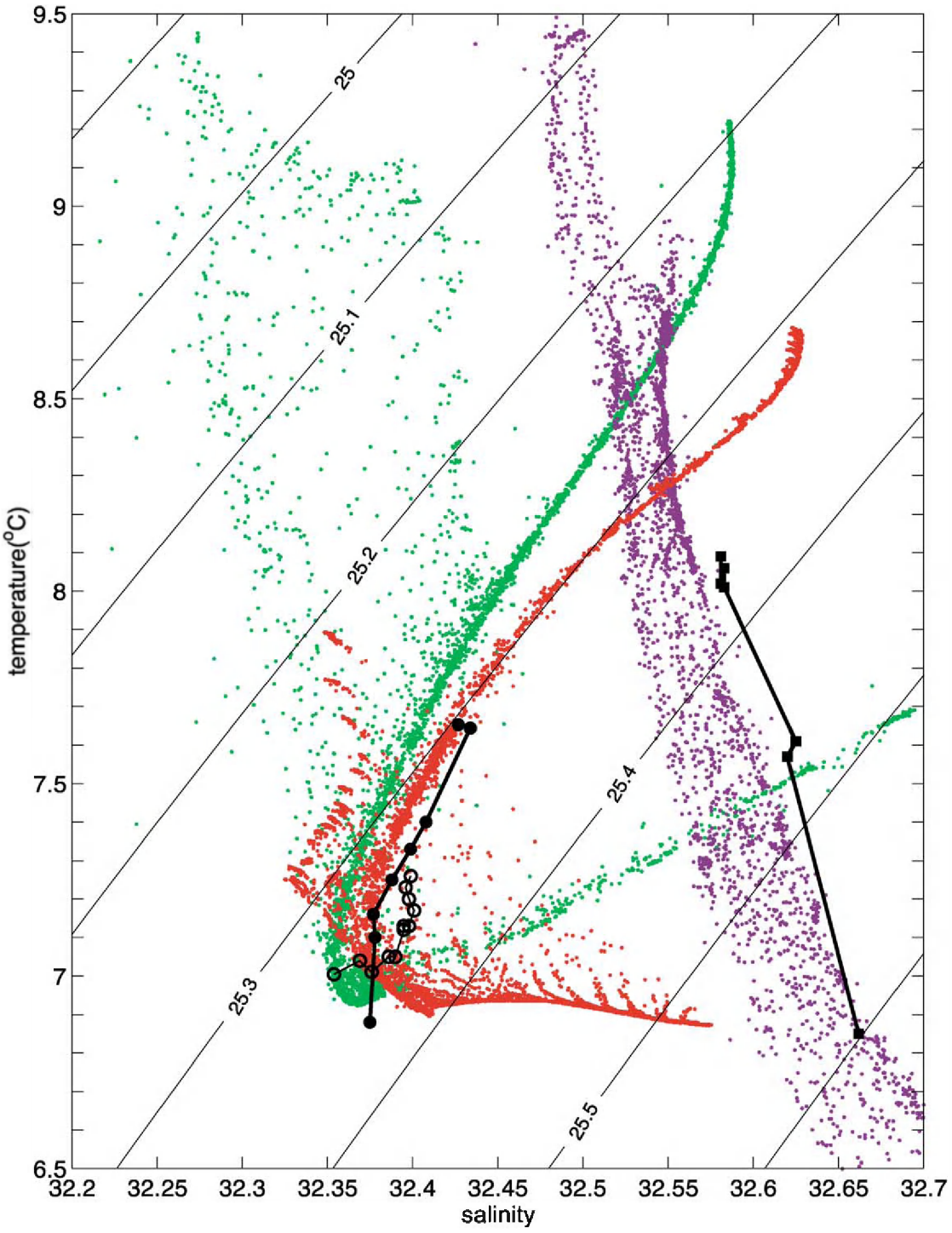

Fig. 6. *T*/*S* distribution of data derived from the preinjection on cross-bank sections, shown in Fig. 2, for #1 (red), #2 (green), and #3 (blue). Superposed are the dye patch averaged *T*/*S* values of #1 (●), #2 (○), and #3 (■).

warming of the water column on the vertically well-mixed side of the tidal front. The *T/S* values of the evolving dye patches follow but are slightly displaced from curves defined by the preinjection surveys due to changes in the local water properties during the intervening time and space interval between the pre-injection survey and the dye injection. For #2, there is a transition from when the patch first moves toward the shelfbreak front, becoming denser, to a later on-bank flow into the tidal front that decreases its density.

3.3. Dye patch temperature distribution

The temperature distribution within the dye patch near the beginning and at the end of each dye deployment is shown in Fig. 7. Patch averaged, dye concentration weighted, temperature distributions are then calculated from an interpolated data grid derived from the position-adjusted sections of the surveys that define the patch. Dye concentrations measured at the deepest point of the Scanfish track were extrapolated to the bottom since it is in the BML. The vertical integration extends only up to 18 m, the base of the surface thermocline, in order to highlight the changes in the temperature of the dye passing laterally through the tidal front and to minimize the effect of heating due to vertical mixing near the surface. Because of the cross-bank shear in the along-shelf flow (the flow is stronger on the off-bank side of the tidal front), there is an along-shelf temperature gradient within the patch. This is especially pronounced for #3 where the trailing end of the patch was warmer since this water had penetrated further across the tidal front.

There is considerable variation in the time evolution of the patch average temperature for each experiment. For #1, the peak at 7.0 °C is significantly warmer than the injection temperature of ~ 6.9 °C 17 h earlier. By 84 h, dye is distributed between 7.0 and 8.9 °C with a patch mean temperature of 7.62 °C. The broad distribution is due in part to the along-front gradient within the patch. On individual cross-frontal sections, the distribution is more peaked over a narrower temperature range. For #2, the temperature distribution is much narrower, since for the first 30 h, the patch was undergoing predominately isothermal displacements in the region between the tidal and shelfbreak fronts. A significant diathermal shift and dispersion only occurred later as the dye patch began to enter the tidal

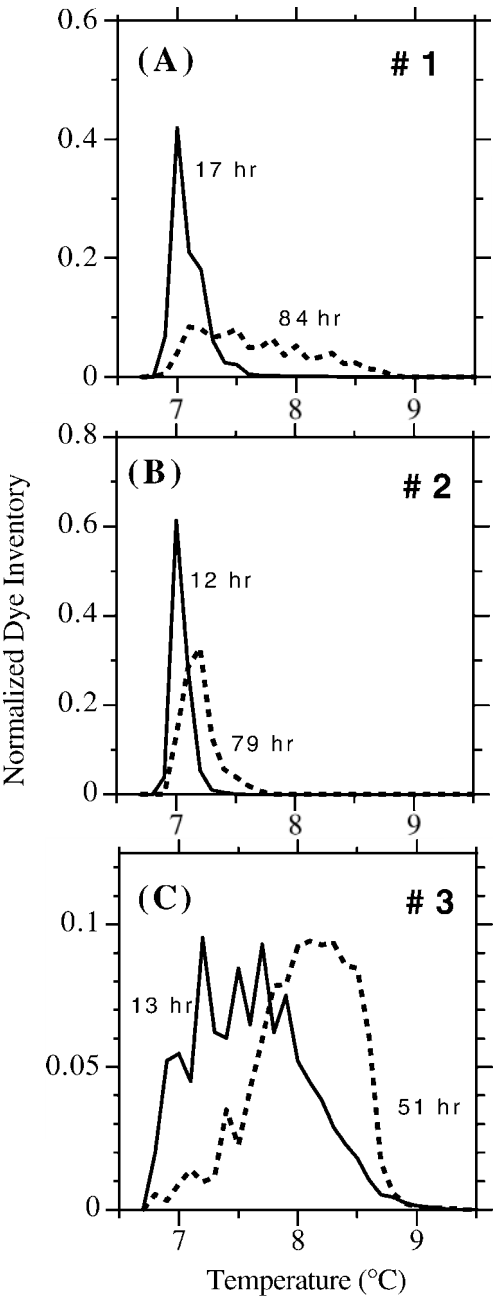

Fig. 7. Dye distribution throughout the patch in 0.1 °C temperature increments of two patch surveys for each injection: #1 (A), #2 (B), and #3 (C). All curves normalized to unit area. Time (hours) from injection for a particular survey is indicated.

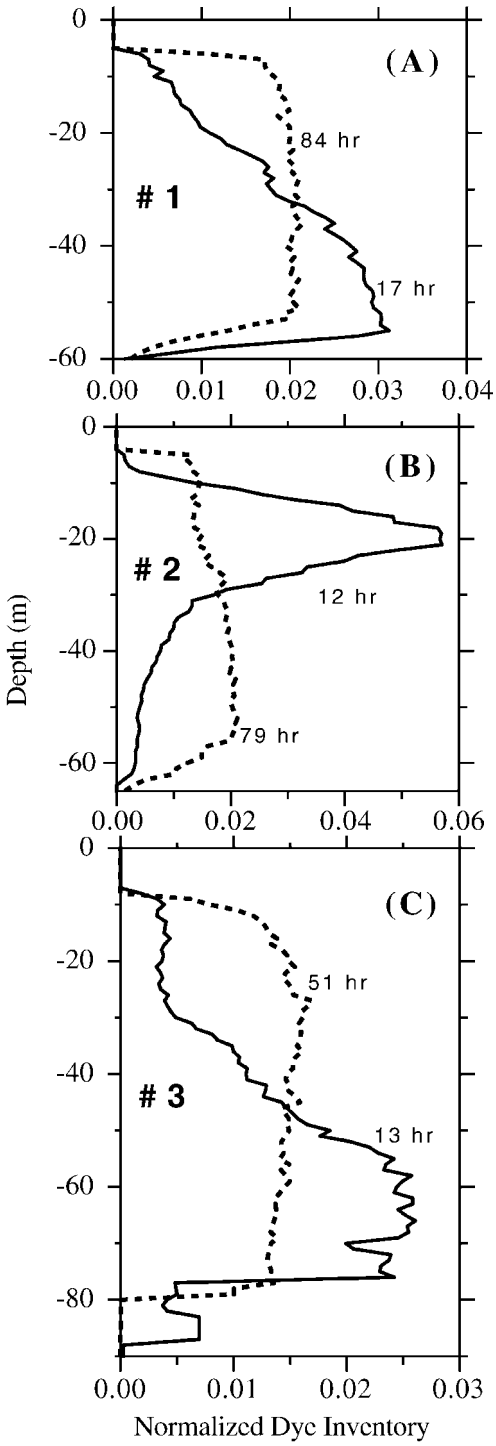

front. For #3, the temperature distribution broadened rapidly because of the more energetic tidal motion of the northeast peak and because the dye injection was well within the tidal front. By 51 h, most of the dye was at temperatures greater than 8.0 °C, i.e., it had passed through the front.

3.4. Dye patch dispersion

The dispersion of the dye patch is illustrated by the vertical (Fig. 8) and lateral (Fig. 9) distribution of the dye within the patch. The vertical distribution is calculated up to 5 m depth, the maximum vertical excursion of the Scanfish. The decreasing dye inventory near the bottom is due to the sloping bottom across the patch. The maximum at 20 m depth in the dye profile for #2 is due to the shoaling event forced by the shelfbreak front incursion. For all three injections, the dye was uniformly mixed throughout the water column by the end of the experiment.

The lateral distribution of the vertically integrated dye is partitioned into a major axis and minor axis. The major axis is defined by the rotated axis that produces maximum variance. The minor axis is then the perpendicular. These are roughly the along-front and cross-front axes, respectively.

4. Results

4.1. Diapycnal velocities

The diapycnal passage of the dye patch through the tidal front is inferred from the changes in its water properties. We use temperature since it is measured with the greatest precision and since temperature gradients across the front are the least ambiguous. Changes in the temperature distribution and, hence, patch mean temperature can be the result of spatial variations of the diffusivity and/or the temperature gradient. However, the fact that hardly any dye remained at the injection temperature suggests that

Fig. 8. Same as Fig. 7 except for the vertical distribution of the dye in 1-m increments. The shape of the depth distribution distorted by the bottom depth changes and the vertical extent of the survey. The irregular distribution at depth for #3 (13 h) is due to under sampling of the dye patch at depth greater than 80 m.

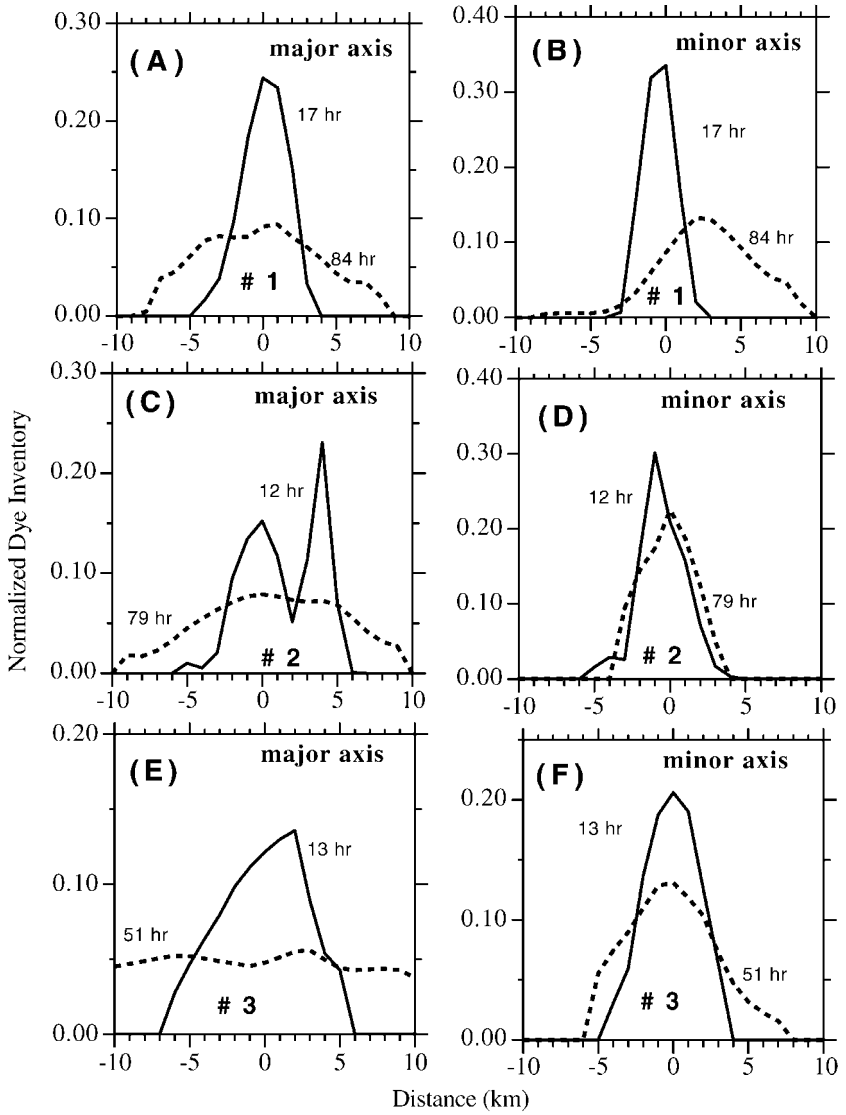

Fig. 9. Same as Fig. 7 except for the lateral distribution of the dye in 1-km increment resolved into the major (along-front) axis and minor (cross-front) axis (see text for definition). In E, the distribution at 51 h is truncated at ± 10 km because the survey did not extend across the entire patch.

the first-order change in the patch mean temperature is due to diapycnal flow and not asymmetric dispersion.

The time dependence of the patch-averaged temperature is shown in Fig. 10. For #1, the warming is roughly linear throughout the experiment. By the time that it has warmed to 7.8 °C, the centroid of the dye patch has passed through the tidal front although warming could continue due to the horizontal temperature gradients within the vertically mixed water on the cap of the bank. For #3, the initial warming is more rapid but then decreases as the centroid of the dye patch has passed through the tidal front into an interior region with weaker horizontal gradients. The temperature change for #2 is more ambiguous. Fig. 6 indicates that for the first 30 h, there was a slight warming and increased density as the patch moved

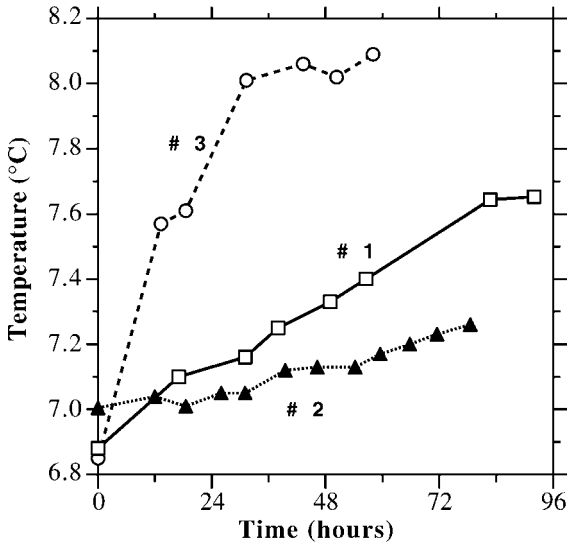

Fig. 10. Time dependence of patch averaged temperatures for #1 (□), #2 (▲), and #3 (○).

off-bank toward the shelfbreak front. The subsequently more rapid warming and density decrease indicate an on-bank flow toward the tidal front.

The motion of the dye patch across the tidal front is inferred from its temperature increase and the cross-bank temperature gradient in the BML observed during the course of the experiment. However, some of the temperature increase is due to the seasonal heating of the water column, i.e., the thermal structure of the front during each dye experiment is not quite steady-state. We estimate the water column warming from the vertical displacement of the preinjection T/S curve of #2 from #1 shown in Fig. 6. Over the T/S interval appropriate to the experiment #1, the average warming is 0.2 °C over a 6-day interval, which implies a 0.12 °C warming during the 3.5 days of experiment #1. We subtract this warming rate, 0.034 °C/day, from the observed warming for each of the three dye experiments.

On the south flank, the observed dye patch #1 temperature increase of $\Delta T = 0.76$ °C over 83 h implies a net warming due to its cross-frontal motion of 0.64 °C or a rate of $\partial T/\partial t = 2.1 \times 10^{-6}$ °C/s. The cross-frontal temperature gradient between 6.8 and 7.7 °C, an average of repeated sections crossing the front, is $\partial T/\partial y = 1.3 \times 10^{-4}$ °C/m. The on-bank cross-frontal displacement of the patch centroid is thus $\Delta y = \Delta T/(\partial T/\partial y) = 4.9$ km with a mean speed $v = \Delta y/\Delta t = 1.6$ cm/s. This is comparable to the speed of 1.4 cm/s derived from a similar calculation using the patch salinity changes and the frontal salinity gradient which, however, is less precise than the temperature calculation. For injection #2, the adjusted net temperature increase of $\Delta T = 0.15$ °C during the last 48 h of the experiment and a mean temperature gradient of $\partial T/\partial y = 1.0 \times 10^{-4}$ °C/m implies an on-bank dispacement of $\Delta y = 1.5$ km and a speed $v = 0.9$ cm/s.

On the northeast peak (#3), we take the net temperature increase $\Delta T = 1.15$ °C in the first 43 h to represent the cross-frontal passage. This rate of warming, $\partial T/\partial t = 7.4 \times 10^{-6}$ °C/s, is more than three times that observed on the south flank. With a mean cross-bank temperature gradient of $\partial T/\partial y = 2.4 \times 10^{-4}$ °C/m, about twice that on the south flank, we infer an on-bank displacement of $\Delta y = 4.8$ km and a mean cross-frontal speed of $v = 3.1$ cm/s. Thus, the mean on-bank Lagrangian flow on the northeast peak is approximately twice that on the south flank. These results are tabulated in Table 2.

The magnitude of the cross-front flow varies within the tidal front. Using the cross-frontal variation of $\partial T/\partial t$ derived from a smooth curve fitted data in Fig. 10 and $\partial T/\partial y$ from a smooth curve fitted to repeated cross-front BBL temperature sections, we calculate $v = (\partial T/\partial t)/(\partial T/\partial y)$ as a function of position within the front (Fig. 11). The on-bank flow is greatest at the off-bank edge of the tidal front and decreases monotonically to effectively zero on the on-bank side. This decrease is consistent with model calculations (Chen et al., in press) consisting of an on-bank flow through the base of the tidal front feeding into upwelling on the stratified side. Thus, the dye tracer data suggest that the on-bank flow in the base of the tidal front does not continue onto the cap of the bank.

Table 2
Cross-frontal velocities

	South flank		Northeast peak
	#1	#2	
Net warming: ΔT (°C)	0.64	0.15	1.15
Duration: Δt (h)	83	48	43
dT/dt ($\times 10^{-6}$ °C/s)	2.1	0.9	7.4
dT/dy ($\times 10^{-4}$ °C/m)	1.3	1.0	2.4
On-bank displacement: Δy (km)	4.9	1.5	4.8
On-bank velocity: v(cm/s)	1.6	0.9	3.1

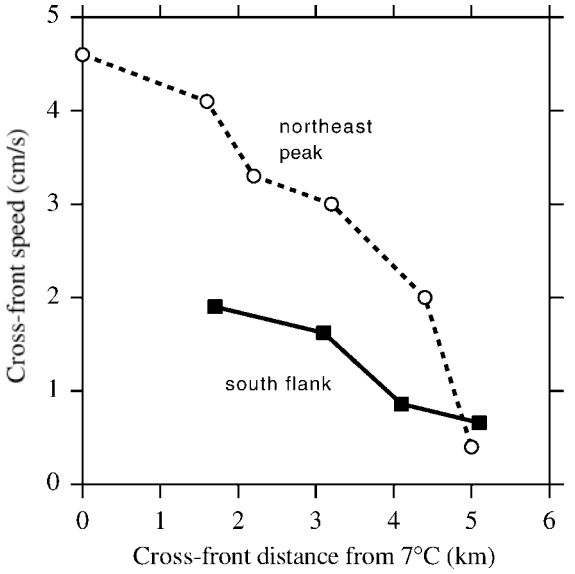

Fig. 11. Cross-front speed as a function of the distance from the location of 7 °C in the BML.

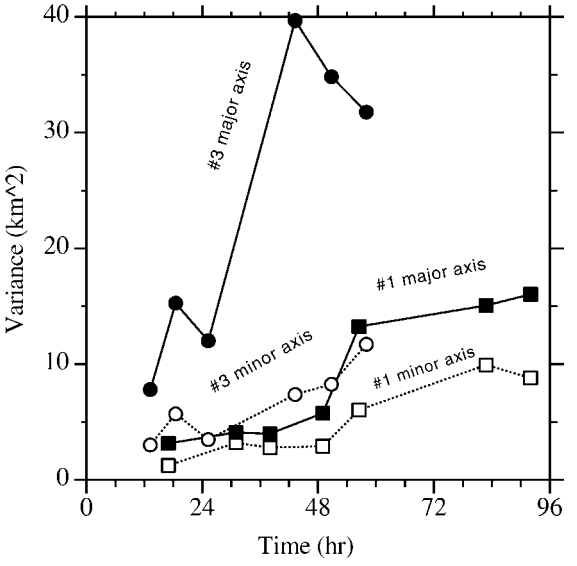

Fig. 12. Same as Fig. 10 except for lateral variance along the major axis (solid) and minor axis (open) for #1 (square) and #3 (circle).

4.2. Temperature flux divergence

As the dye-tagged water passes through the quasi-steady-state temperature gradient of the tidal front, there must be sufficient heat flux divergence to account for its warming. In the Lagrangian reference frame of the patch

$$\mathrm{d}T/\mathrm{d}t = \partial/\partial z(K_z \partial T/\partial z) + \partial/\partial y(K_y \partial T/\partial y) \approx K_z \partial^2 T/\partial z^2 + K_y \partial^2 T/\partial y^2 \quad (1)$$

where y is the cross-front axis and we omit the so-called pseudo-advection terms $\partial K_z/\partial z \partial T/\partial z$ and $\partial K_y/\partial y \partial T/\partial y$. We apply this equation in a patch average sense assuming constant diffusivities as a rough diagnostic to compare the dye patch warming with an estimate of the local temperature flux divergence.

The cross-front diffusivity, K_y, is estimated from the time dependence of the lateral variance of the dye patch (Fig. 12) vertically integrated from the bottom up to 18 m depth. The lateral variance is partitioned into the major axis and minor axis, which are essentially equivalent to the along-front and cross-front components. There is considerable uncertainty in these variance calculations because, in part, the appropriate velocity field required to adjust the data position is uncertain, a survey occasionally failed to define the along-front ends of the patch, and the dye inventory decreased near the end of a survey as a greater proportion of the dye was diluted to concentrations below detectable levels.

We estimate the diffusivity by fitting the variance to a linear regression (a Fickian model) between 18 and 84 h for #1 and between 12 and 48 h for #3. The error associated with this diffusivity estimate is especially difficult to quantify. However, to estimate the error, a range of possible slopes were fitted to the data points excluding those whose large deviation from a smooth curve can be attributed to a specific sampling problem. The magnitude of these deviations gives a rough indication of the error in the individual variance calculation. The range of slopes thus fitted yields an uncertainty of approximately 25% to the values tabulated in Table 3.

Table 3
Tidal front diffusivities

	South flank	Northeast peak
Along-front (m^2/s)	28	116
Cross-front, K_y (m^2/s)	18	30
Vertical, K_z ($\times 10^{-3}$ m^2/s)	1.4	2.5

For the vertical diffusivity, K_z, we use the time dependence of the patch average vertical variance (Fig. 13) calculated from the bottom up to 18 m depth, i.e., through the bottom mixed layer up to the base of the thermocline where the buoyancy frequency is approximately 3×10^{-3} rad/s. For both the south flank and northeast peak, the variance increases approximately linearly for the first 24 h before becoming roughly constant as the patch has mixed uniformly up to the base of the summer pycnocline. Again, using a Fickian model fitted to the first 24 h and estimating the error for the individual data points from the fluctuations of the subsequent variance calculations, we get $K_z = 1.4$ and 2.5×10^{-3} m^2/s on the south flank and northeast peak, respectively, with an uncertainty of approximately 20%.

These diffusivities are combined with estimates of the temperature gradients to evaluate the temperature flux divergence terms in Eq. (1). Because of the considerable scatter among the individual temperature sections, an ensemble average of all cross-front sections taken in the course of surveying the patch is used to construct average temperature gradients. In the BML of the tidal front between 7 and 7.5 °C on the south flank, $\partial^2 T/\partial y^2$ is approximately 0.39×10^{-7} °C/m^2. With $K_y = 18$ m^2/s, this implies a lateral temperature flux divergence $K_y \partial^2 T/\partial y^2 = 0.7\,°\text{C} \times 10^{-6}$ °C/s or about 30% of the observed flux into the dye patch. On the northeast peak, the inflection point of the temperature gradient, i.e., where $\partial^2 T/\partial y^2 = 0$, is at 7.5 °C. Since d$T$/d$y$ is approximately constant from 6.8 to 8.2 °C, the dye patch is in a region where $\partial^2 T/\partial y^2 \approx 0$ and the lateral temperature flux divergence is negligible. Thus, the cross-bank temperature flux divergence makes at most only a minor contribution to the observed warming of the dye patch within the tidal front on both the south flank and the northeast peak.

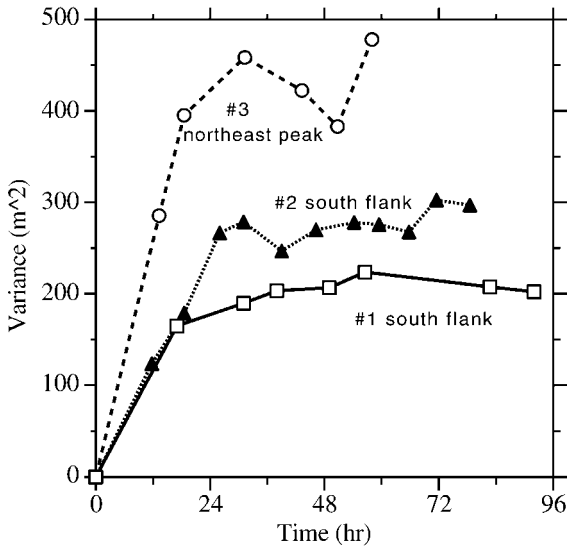

Fig. 13. Same as Fig. 10 except for vertical variance.

The vertical temperature flux divergence is estimated in a similar way. Because of the vertical temperature gradient changes across the tidal front, it is difficult to estimate the $\partial^2 T/\partial z^2$ that is appropriate for the dye patch as it passes through the tidal front in the course of the experiment. Taking the difference between a mean $\partial T/\partial z$ in the BML and at the base of the thermocline, where the buoyancy frequency is approximately 12×10^{-3} rad/s, from repeated temperature profiles, we get $\partial^2 T/\partial z^2 = 2$ and 4×10^{-3} °C/m^2 on the south flank and northeast peak, respectively. The uncertainty in this calculation is particularly difficult to estimate. Across the tidal front, $\partial^2 T/\partial z^2$ varies by a factor of 4. The values given above are biased to the profiles on the stratified side of the tidal front. This presumably is the location of the dye patch during the period of rapid vertical dispersion used to estimate K_z. Combining these with diffusivities of $K_z = 1.4$ and 2.5×10^{-3} m^2/s, we have a temperature flux divergence $K_z \partial^2 T/\partial z^2 = 2.8$ and 10.0×10^{-6} °C/s on the south flank and northeast peak, respectively. These values are comparable to patch warming rates of 1.9 and 7.6×10^{-6} °C/s on the south flank and northeast peak. Although the level of agreement is certainly fortuitous, it strongly suggests that the warming of the dye patch within the tidal front is due predominantly to vertical mixing of heat.

5. Discussion

5.1. Cross-front flow

These results provide the first opportunity to test model predictions of the cross-frontal exchange. An earlier study by Loder and Wright (1985) suggested Lagrangian cross-bank speeds in the range of

1–2 cm/s. A more recent study (Chen et al., in press) used a 3-D primitive equation model with level 2.5 Mellor–Yamada turbulent closure, climatological stratification, and wind and M_2 tide forcing. They calculated 30-day trajectories of Lagrangian particles released at the bottom on the south flank at the 60 m and terminating at the 40 m isobath with a mean on-bank speed of 1.4 cm/s. Particles released at the 140 m isobath at the northeast peak shoaled to 10 m depth over the bank 30 days later for a mean on-bank speed of 2.7 cm/s. Although these trajectories are not equivalent to our dye patch displacements, the similarity of the speeds is striking though perhaps fortuitous.

The difference in the evolution of injections #1 and #2 suggest significant temporal and spatial variations in the flow field. The two injections on the south flank were virtually in the same location with respect to the tidal front but #2 was in a cross-bank temperature minimum because of the proximity of the shelfbreak front offshore. A convergent flow toward the foot of this front has been modeled by Chapman and Lentz (1994) and observed by Houghton (1997) and Houghton and Visbeck (1998). The initial isothermal shoaling of #2 (Fig. 5c) suggests a complex 3-D circulation associated with the intruding shelfbreak front. Its subsequent increasing salinity and density while the temperature remained virtually constant (Fig. 6) implies a patch displacement toward the shelfbreak front. The more rapid increase in temperature and decrease in density after 31 h indicate a patch displacement toward the tidal front. These results suggest that there is a divergence in the near bottom cross-bank flow between the tidal and shelfbreak fronts consistent with modeling results by Chen et al. (in press).

For mass continuity, we expect a compensating off-bank flow in the upper water column at the tidal front. Model studies by Chen and Beardsley (1998) and Chen et al. (in press) produce a Lagrangian residual cross-bank circulation consisting of on-bank flow in the lower water column, upwelling on the mixed side of the front, and off-bank flow in the upper third of the water column that then subsides beneath the pycnocline on the stratified side of the front. There is no evidence of a near surface off-bank flow during experiment #1. The distribution of the dye, even when mixed uniformly to 10 m depth (Fig. 5b), has no off-bank displacement near the surface. Perhaps the off-bank flow is confined to the upper 10 m or incorporated in circulation with 3-D structure.

In experiment #3, the upper portion of the dye patch (Fig. 5f) is displaced off-bank into the pycnocline suggesting off-bank flow there. The dye, initially injected near the bottom, passed through the tidal front then mixed to the surface in the interior region with weaker lateral gradients. The upper portion of the dye patch then protrudes off-bank into the pycnocline. Whether this protrusion is due to a mean off-bank Lagrangian flow or just enhanced isopycnal mixing in the pycnocline is not clear. However, the dye in the pycnocline at mid-depth at the edge of the bank apparently did not get there by direct vertical mixing from the injection location below but via the on-bank flow through the front, the vertical mixing in the interior of the bank and then the off-bank flow or isopycnal dispersion at mid-depth. It is the short time scales of these processes compared to direct vertical mixing that make the role of this secondary circulation in the vertical exchange across the pycnocline discernable in the data.

5.2. Cross-front heat exchange

The on-bank flow through the tidal front provides a mechanism for cross-frontal exchange. We consider here the contribution of this exchange to the heat budget on the bank. The possibility of heat export from the cap of Georges Bank was first suggested by Loder et al. (1982), who noted that the climatological surface heat input calculated by Bunker (1976) implied a summertime increase in SST about twice that observed. From a model fit to the observed lateral thermal structure, they infer horizontal diffusivities of 150–380 m^2/s on the cap of the bank. The temperature gradients observed inside the tidal front (Fig. 3a) supports the notion of an off-bank heat flux.

In order to make a crude but quantitative estimate of the heat flux, we model the bottom depth on the cap of Georges Bank, following Loder et al. (1982), as an axisymmetric cone with a water depth of 10 m at the center and 43 m at the 45-km radius which is constructed such that the surface area inside each depth contour closely approximates that estimated

from bathymetric charts. We take this to represent the well-mixed portion of the bank inside the tidal front. Hydrographic data from the monthly GLOBEC broad-scale surveys indicate that this water warmed at a rate of 1×10^{-6} °C/s during May and June 1999, which is equivalent to a heat increase of 8.6×10^{11} W. The climatological surface heat flux calculated from COADS data (Beardsley, personal communication) is approximately 190 W/m^2, equivalent to a warming of 12.1×10^{11} W. However, a 5-year record of heat flux using GLOBEC south flank long-term mooring data (courtesy of J. Irish and R. Beardsley, personal communication) shows interannual fluctuations of the flux that range over an interval of 100 W/m^2. They also show that during the spring of 1999, the surface heat flux was above the record average. So, if we take the surface heat flux to be in the range of 200–230 W/m^2, then the excess heat to be exported is approximately $4–6 \times 10^{11}$ W.

We estimate the cross-bank heat flux implied by the dye patch velocity measurements in the following way. Consider a boundary around the bank situated on the seaward, stratified, side of the tidal front. In our axisymmetric model with a tidal front 5-km wide this would be a cylinder with radius of 50 km. We approximate the net cross-bank heat flux with a bottom slab 30 m thick of 7 °C water moving on-bank at 2 cm/s with a surface layer of 8 °C water with the same flux moving off-bank. The net horizontal heat flux off the bank is then 8×10^{11} W, a value with the same order of magnitude as our estimate of the required heat export from the cap of the bank.

6. Conclusions

With a dye tracer, we have observed an on-bank diapycnal Lagrangian flow in the BML through the tidal front of 1.6 cm/s on the south flank and 3.1 cm/s on the northeast peak. The cross-bank flow appears to terminate at the vertically well-mixed side of the front. This result, consistent with recent model predictions (Chen et al., in press), could never have been obtained with Eulerian measurements, especially in such an energetic tidal regime. Tracer technologies are essential to measure this cross-frontal flow.

From the dispersion of the dye patches, we obtain vertical diffusivities of 1.4 and 2.5×10^{-3} m^2/s and cross-frontal diffusivities of 18 and 30 m^2/s within the tidal front on the south flank and northeast peak of Georges Bank, respectively. It is predominantly vertical mixing within the front that affects the required property changes in the water column as dye-tagged water flows diapycnally through the front.

Summertime satellite (SST) images (Loder et al., 1982; Bisagni et al., 2001) show an annulus of cold water surrounding the cap of Georges Bank. There is evidence of this feature in our cross-bank sections (Fig. 2a and b). This is a signature of the tidal front. The vigorous vertical mixing there mixes heat into the cold water upwelled onto the bank in the BML. Thus, the available reservoir of cold water at depth is greater than that implied by the thickness of the water column at the front. The rate of warming of the dye patch implies a downward flux of heat within the tidal front of approximately 300 W/m^2, which is comparable in magnitude to the surface heat flux. It is evident that the observed cross-front flow plays a significant role in the Georges Bank heat budget and thermal structure.

Acknowledgements

The success of this cruise is due to the skill and patience of Captain Bearse and the crew of the R/V OCEANUS. Special thanks is given to Jay Ardai who maintained the dye injection and detection systems, to Dave Nelson who operated the Scanfish provided by the University of Rhode Island, to C. Ho for data analysis and figure preparation, to Martin Visbeck for helpful discussions, and to anonymous reviewers for their constructive critical comments. This project is supported by NSF grant OCE9806361. Lamont Doherty Earth Observatory contribution no. 6376 and U.S. Western North Atlantic GLOBEC Program No. 353.

References

Bisagni, J.J., Seemann, K.W., Mavor, T.P., 2001. High-resolution satellite-derived sea surface temperature variability over the Gulf of Maine and Georges Bank region, 1993–1996. Deep-Sea Res., Part II 48, 71–94.

Bunker, A.F., 1976. Computations of surface energy flux and annual air–sea interaction cycles of the North Atlantic Ocean. Mon. Weather Rev. 104, 1122–1140.

Butman, B., Beardsley, R.C., 1987. Long-term observations on the southern flank of Georges Bank: Part I. A description of the seasonal cycle of currents, temperature, stratification, and wind stress. J. Phys. Oceanogr. 17, 367–384.

Chapman, D.C., Lentz, S.J., 1994. Trapping of a coastal density front by the bottom boundary layer. J. Phys. Oceanogr. 24, 1465–1479.

Chen, C., Beardsley, R.C., 1998. Tidal mixing and cross-frontal particle exchange over a finite amplitude asymmetric bank: a model study with application to Georges Bank. J. Mar. Res. 56, 1163–1201.

Chen, C., Beardsley, R.C., Limeburner, R., 1995. A numerical study of stratified tidal rectification over finite-amplitude banks: Part II. Georges Bank. J. Phys. Oceanogr. 25, 2111–2128.

Chen, C., Beardsley, R.C., Franks, P.J.S., 2002. Model study of the cross-frontal water exchange on Georges Bank: a 3-D Lagrangian experiment. J. Geophys. Res. (in press).

Garrett, C.J.R, Loder, J.W., 1981. Dynamical aspects of shallow sea fronts. Philos. Trans. R. Soc. Lond., A 302, 563–581.

Garrett, C.J.R., Keely, J.R., Greenberg, D.A., 1978. Tidal mixing versus thermal stratification in the Bay of Fundy and Gulf of Maine. Atmos.-Ocean 16, 403–423.

Houghton, R.W., 1997. Lagrangian flow at the foot of a shelfbreak front using a dye tracer injected into the bottom boundary layer. Geophys. Res. Lett. 24, 2035–2038.

Houghton, R.W., Visbeck, M., 1998. Upwelling and convergence in the Middle Atlantic Bight shelfbreak front. Geophys. Res. Lett. 25, 2765–2768.

Limeburner, R., Beardsley, R.C., 1996. Near surface recirculation of Georges Bank. Deep-Sea Res., Part II 43, 1547–1574.

Loder, J.W., Wright, D.G., 1985. Tidal rectification and frontal circulation on the sides of Georges Bank. J. Mar. Res. 43, 581–604.

Loder, J.W., Wright, D.G., Garrett, C., Juszko, B.-A., 1982. Horizontal exchange on central Georges Bank. Can. J. Fish. Aquat. Sci. 39, 1130–1137.

Loder, J.W., Brinkman, D., Horne, E.P.W., 1992. Detailed structure of currents and hydrography on the northern side of Georges Bank. J. Geophys. Res. 97, 14331–14351.

Lynch, D.R., Ip, J.T.C., Naimie, C.E., Werner, F.E., 1996. Comprehensive coastal circulation model with application to the Gulf of Maine. Cont. Shelf Res. 16, 875–906.